International Journal of Thermophysics, Vol. 25, No. 3, May 2004 (© 2004)

A Thermodynamic Equation of State for the Critical Region of Ethylene

A. Abbaci[1,2] **and A. Berrezeg**[1]

Received June 23, 2003

A fundamental equation of state that describes the behavior of the thermodynamic properties of ethylene in the vicinity of the critical point is formulated. Specifically, a crossover equation of state that takes into account not only the scaling laws at the critical point but also the analytical behavior far away from the critical point is presented. Analysis of different sets of data for the thermodynamic properties is made.

KEY WORDS: critical parameters; equation of state; ethylene; sound velocity; specific heat; thermodynamic properties.

1. INTRODUCTION

Ethylene is a very important fluid due to its useful applications in industry. It is an important alkene in several olefins and is a key substance that enters into the production of ethanol, polyethylene, polystyrene, and high-efficiency liquid fuels.

The work described in this paper is part of a research effort to develop a comprehensive fundamental equation for the thermodynamic properties of ethylene. The proposed equation of state is not only valid in the vicinity of the critical region but is also capable of describing the thermodynamic properties of ethylene analytically far away from the critical region. An analytic equation, such as the one proposed by McCarty and Jacobsen [1], is not suitable for an accurate representation of the thermodynamic properties of fluids in the near-critical region, and it became

---

[1] Faculté des Sciences, Département de Chimie, Université Badji-Mokhtar B.P. 12, El-Hadjar, Annaba (23200), Algeria.

[2] To whom correspondence should be addressed. E-mail: abbaci_a2002@yahoo.fr

our task to supplement the global equation of state with an equation of state for the near-critical region. For this purpose, Olchowy and coworkers [2, 3] made an attempt to represent the thermodynamic properties of ethylene in the near-critical region with the aid of the so-called revised and extended scaled parametric equation of state [4, 5]. The problem with the scaled equations of state is that they are only valid in a limited range of densities and temperatures around the critical point [5]. This restriction becomes particularly severe at temperatures below the critical temperature.

The development of our equation of state was based on P–ρ–T data (P is pressure, ρ is density, and T is temperature) reported by Nowak et al. [6] since they provide adequate P–ρ–T information in the near-critical region as well as in the far away region. It is then possible to obtain a global equation of state in the near-critical region that represents the P–ρ–T data of Nowak et al. [6] and the speed-of-sound C_s data of Gammon [7]. Comparisons with different sets of P–ρ–T data from different sources show good agreement with the data of Nowak et al. [6], and have also revealed good agreement between the speed-of-sound data measured by Gammon [7] and the speed of sound reported by Dregulyas and Stavtsev [8] and the isobaric specific-heat data of Hejmadi and Powers [9].

Chen et al. [10, 11] have developed a new theoretically based equation of state for fluids in the critical region that incorporates the crossover from the scaled thermodynamic behavior asymptotically close to the critical point to the analytic classical thermodynamic behavior far away from the critical point. They verified that their crossover model yields an accurate representation of the thermodynamic properties of several fluids in the critical region covering a large range of densities and temperatures around the critical point and extending into the far-critical region where analytic equations of state should be accurate [12]. Hence, we decided to apply this crossover model to ethylene.

For this purpose, we shall describe our new theoretically based crossover equation of state in Section 2. In Section 3, we discuss its application to ethylene and use it to analyze the available experimental data for C_2H_4 in the critical region.

2. FUNDAMENTAL EQUATION

Asymptotically close to the critical point, the thermodynamic properties of fluids satisfy scaling laws with universal critical exponents and universal scaling functions [4, 13]. Equations of state for fluids incorporating these scaling laws have been developed earlier. In a previous work, a linear-model parametric equation of state was revised to include vapor–liquid asymmetry and extended to incorporate the first corrections beyond asymptotic scaling [5, 14–16]. The range of validity of such a scaled equation of state is still somewhat restricted, and the agreement with the experimental data deteriorates very rapidly as soon as the scaled equation is extrapolated outside the near-critical region. On the other hand, outside the critical region, the thermodynamic properties can be adequately represented by classical equations that are analytic everywhere. In order to combine the scaling laws near the critical point with classical equations, one needs to use a certain mechanism that includes the crossover from scaled behavior near the critical point to analytic behavior far away from the critical point.

Starting from the earlier work of Nicoll et al. [17–19], we have developed a crossover model to represent the thermodynamic properties of fluids in the critical region [11, 12]. This crossover model is based on the renormalization group theory of critical phenomena to include the cooperative effects associated with the long-range critical fluctuations up to a maximum microscopic wave number.

Let ρ be the density, T the temperature, P the pressure, μ the chemical potential, and A/V the Helmholtz free energy per unit volume. We make these properties dimensionless with the aid of the critical parameters [4]:

$$\tilde{\rho}=\frac{\rho}{\rho_c},\ \tilde{T}=-\frac{T_c}{T},\ \ \tilde{P}=\frac{PT_c}{P_cT},\ \ \tilde{\mu}=\frac{\mu\rho_cT_c}{P_cT},\ \ \tilde{A}=\frac{AT_c}{P_cVT}. \tag{1}$$

In addition we define

$$\Delta\tilde{\rho}=\tilde{\rho}-1,\ \ \Delta\tilde{T}=\tilde{T}+1,\ \ \Delta\tilde{\mu}=\tilde{\mu}-\tilde{\mu}_0(\tilde{T}), \tag{2}$$

and

$$\Delta\tilde{A}=\tilde{A}-\tilde{\rho}\tilde{\mu}_0(\tilde{T})-\tilde{A}_0(\tilde{T}). \tag{3}$$

Here, $\tilde{\mu}_0(T)$ and $\tilde{A}_0(T)$ are analytic background functions of T subject to the conditions that $\Delta\tilde{\mu}=0$ and $\tilde{A}_0=1$ at the critical temperature. The relevant thermodynamic relations in terms of these reduced thermodynamic properties can be found elsewhere [11, 12].

Classical equations of state for the Helmholtz free energy density A imply that the classical part A_{cl} has an asymptotic expansion of the form,

$$\Delta\tilde{A}_{cl}=\frac{1}{2}tM^2+\frac{u_0}{2!}M^4+\cdots, \tag{4}$$

where t and M are temperature-like and density-like variables related to ΔT and $\Delta\rho$ in a manner to be specified below. In the following, we find it convenient to write the coefficient u_0 of the M^4 term in Eq. (4) as

$u_0 = \Lambda u$, where Λ is a dimensionless cutoff wave number [10]. In order to obtain a fundamental equation that can be applied in a large range of densities and temperatures around the critical point, we retain six terms in the classical Landau expansion (4) for ΔA_{cl}

$$\Delta\tilde{A}_{\mathrm{cl}} = \frac{1}{2}tM^2 + \frac{u_0}{2!}M^4 + \frac{a_{05}}{5!}M^5 + \frac{a_{06}}{6!}M^6 + \frac{a_{14}}{4!}tM^4 + \frac{a_{22}}{2!2!}t^2M^2. \tag{5}$$

As shown by Chen et al. [10], the theoretically predicted asymptotic behavior can be recovered from this expansion by the following transformation:

$$\begin{aligned}\Delta\tilde{A}_r = {} & \frac{1}{2}tM^2\mathsf{T}\mathsf{D} + \frac{u_0}{2!}M^4\mathsf{D}^2\mathsf{U} + \frac{\mathrm{a}_{05}}{5!}M^5\mathsf{D}^{5/2}\mathsf{V}\mathsf{U} + \frac{\mathrm{a}_{06}}{6!}M^6\mathsf{D}^3\mathsf{U}^{3/2} \\ & + \frac{\mathrm{a}_{14}}{4!}tM^4\mathsf{T}\mathsf{D}^2\mathsf{U}^{1/2} + \frac{\mathrm{a}_{22}}{2!2!}t^2M^2\mathsf{T}^2\mathsf{D}\mathsf{U}^{-1/2} - \frac{1}{2}t^2\mathsf{K},\end{aligned} \tag{6}$$

where the functions T, D, U, V and K are defined by

$$\begin{aligned}&\mathsf{T} = Y^{(2-1/\nu)/\omega}, \quad \mathsf{D} = Y^{-\eta/\omega}, \quad \mathsf{U} = Y^{1/\omega} \\ &\mathsf{V} = Y^{(2\omega_{\mathrm{a}}-1)/2\omega}, \quad \mathsf{K} = \frac{\nu}{\alpha\bar{u}\Lambda}\left[Y^{-\alpha/\nu\omega} - 1\right].\end{aligned} \tag{7}$$

In terms of a crossover function, Y is to be determined from

$$1 - (1-\bar{u})Y = \bar{u}\left(1 + \frac{\Lambda^2}{\kappa^2}\right)^{1/2} Y^{1/\omega} \tag{8}$$

with

$$\kappa^2 = t\mathsf{T} + \frac{1}{2}u\Lambda M^2\mathsf{D}\mathsf{U}, \tag{9}$$

and

$$\bar{u} = \frac{u}{u^*}. \tag{10}$$

In these expressions ν, η, ω, and ω_{a} are universal critical exponents, and u^* is also a universal constant. The values of the universal critical-region parameters are specified in Table I.

The crossover model depends parametrically on the variable κ^2 defined by Eq. (9). For small values of κ one recovers from Eq. (6) the scaled critical behavior, while for large values of κ the crossover function Y approaches unity and Eq. (6) reduces to the classical Landau expansion of Eq. (5).

Table I. Universal Critical Region Constants

$\nu = 0.630$
$\eta = 0.033$
$\alpha = 2\text{-}3$
$\nu = 0.110$
$\Delta = 0.51$
$\omega_a = 2.1$
$u^* = 0.472$

In order to apply the crossover model to fluids, we need to introduce a proper translation to fluid variables [12]. This is accomplished by the transformation [10–13],

$$\Delta\tilde{A} = \Delta\tilde{A}_r - c\left(\frac{\partial\tilde{A}_r}{\partial M}\right)_t\left(\frac{\partial\tilde{A}_r}{\partial t}\right)_M, \tag{11}$$

$$t = c_t\Delta\tilde{T} + c\left(\frac{\partial\Delta\tilde{A}_r}{\partial M}\right)_t, \tag{12}$$

$$M = c_\rho(\Delta\tilde{\rho} - d_1\Delta\tilde{T}) + c\left(\frac{\partial\Delta\tilde{A}_r}{\partial t}\right)_M, \tag{13}$$

where c, c_t, c_ρ, and d_1 are system-dependent constants. Finally, the total Helmholtz free-energy density is obtained from Eq. (3) as

$$\Delta\tilde{A} = \tilde{A} - \tilde{\rho}\mu_0(\tilde{T}) - \tilde{A}_0(\tilde{T}), \tag{14}$$

with

$$\tilde{\mu}_0(\tilde{T}) = \sum_{j=1}^{j=4}\tilde{\mu}_j(\Delta\tilde{T})^j \text{ and } \tilde{A}_0(\tilde{T}) = -1 + \sum_{j=1}^{j=4}\tilde{A}_j(\Delta\tilde{T})^j. \tag{15}$$

The pressure is deduced from Eq. (15) as

$$\tilde{P} = \Delta\tilde{\mu} + \Delta\tilde{\rho}\Delta\tilde{\mu} - \Delta\tilde{A} - \tilde{A}_0(\tilde{T}). \tag{16}$$

A complete set of equations specifying the crossover model can be found elsewhere [11, 12].

3. APPLICATION TO ETHYLENE

The crossover model as applied to ethylene contains the following system-dependent parameters: the critical parameters T_c, ρ_c, and P_c to be deduced either from an asymptotic analysis of the thermodynamic property data near the critical point or reported by several experiments; the crossover parameters $\bar{u}$ and Λ; the scaling-field parameters c, c_t, c_ρ, and d_1 and the background parameters $\tilde{A}_j$ which can be determined by fitting the crossover model to the P–ρ–T data; and finally the caloric background $\tilde{\mu}_i$ which can be determined from experimental speed-of-sound data or specific-heat data. Actually, the coefficients $\tilde{\mu}_0$ and $\tilde{\mu}_1$ are related to the zero-point values of energy and entropy and are not considered here. The values of the system-dependent parameters adopted for C_2H_4 in this work are presented in Table II. The range of validity of our crossover equation is determined by

$$\tilde{\chi}^{-1} \leqslant 2.2, \tag{17}$$

with the additional restriction that the temperature T should be within the range

$$279\,\mathrm{K} \leqslant T \leqslant 340\,\mathrm{K}, \tag{18}$$

and the density ρ within the range,

$$4.28\,\mathrm{mol}\cdot L^{-1} \leqslant \rho \leqslant 12.94\,\mathrm{mol}\cdot L^{-1} \tag{19}$$

A survey of the available experimental information for the thermodynamic properties of ethylene is contained in the technical report of Olchowy et al. [3] and the papers of Nowak et al. [6] and Smukala et al. [20]. The primary experimental information for developing a thermodynamic surface in the critical region is provided by the P–ρ–T data reported by Nowak et al. [6] from which the system-dependent parameters of the equation of state were determined, and those of Hastings et al. [21] for a 99.993% pure sample. Additional P–ρ–T data have been reported by Douslin and Harrison [22], Trappeniers et al. [23], Michels and Geldermans [24], and Thomas and Zander [25].

In order to determine the values of the system-dependent parameters in the crossover model, we fitted the model to the experimental P–ρ–T data reported by Nowak et al. [6].

First a decision must be made about the values of the critical parameters. A survey of the critical-parameter values reported for C_2H_4 is also included in the technical report of Olchowy co-worker [3] and the work

Table II. System-Dependent Constants for C_2H_4

Critical parameters	$T_c = 282.35$ K
	$P_c = 5.0418$ MPa
	$\rho_c = 7.6367$ mol · L^{-1}
Crossover parameters	$\bar{u} = 0.3682$
	$\Lambda = 1.813$
Scaling-field parameters	$c_t = 1.856$
	$c_\rho = 2.431$
	$c = -0.0344$
Pressure background parameters	$\tilde{A}_0 = -1$
	$\tilde{A}_1 = -5.3525$
	$\tilde{A}_2 = 4.8836$
	$\tilde{A}_3 = 3.7453$
	$\tilde{A}_4 = -7.8945$
	$d_1 = -0.3317$
Classical parameters	$a_{05} = -0.1405$
	$a_{06} = 0.9934$
	$a_{14} = 0.2289$
	$a_{22} = 0.2077$
Caloric background parameters	$\tilde{\mu}_2 = 13.143$
	$\tilde{\mu}_3 = -2.642$

of Nowak et al. [6]. The critical temperature and density of ethylene were reported earlier by Moldover [26] by a visual observation method measurement. As mentioned by Olchowy co-workers [3], a small calibration error was found in the measurements of the vapor pressure using the apparatus of Hastings et al. [21]; as a consequence, we disregard the critical pressure of Moldover. The critical parameters deduced by Olchowy co-workers [3] from the analysis of P–ρ–T of different sources, and those reported by Douslin and Harrison [22] as well as those reported by Nowak et al. [6] are closely related except for the critical density of the latter which is slightly higher than that of Olchowy et al. and that of Douslin and Harrison. The critical parameters we retained for the formulation of our equation of state are the recent finding of Nowak et al. [6]. The different values of the critical parameters are reported in Table III.

Fitting the same crossover equation of state to the P–ρ–T data of Nowak et al. [6] with the critical parameters chosen to be those of the same authors [6], we obtained the system-dependent parameters, such as the crossover parameters, Λ, $\bar{u}$, the scaling-field parameters c_t, c_ρ, c, the classical parameters a_{05}, a_{06}, a_{14}, a_{22}, and the pressure-background parameters $\tilde{A}_1$, $\tilde{A}_2$, $\tilde{A}_3$, and $\tilde{A}_4$. The crossover model fits the P–ρ–T

Table III. Critical Parameters of Ethylene

Author	Data source	T_c (K)	P_c (MPa)	$\rho(\mathrm{mol \cdot L^{-1}})$
Moldover [26]	([a])	282.344 ± 0.0044		7.650 ± 0.021
Douslin and Harrison [22]	PVT [22]	282.35	5.0420	7.635 ± 0.006
Olchowy Co-workers [3]	PVT [21]	282.3452	5.0403	7.634
Nowak et al. [6]	PVT [6]	282.350 ± 0.010	5.0418 ± 0.0011	7.6367 ± 0.0036

[a] Visual observation of meniscus disappearance.

data of Nowak et al. [6] with static $\chi^2 = 2.1$ in the range bounded by Eqs. (17)–(19), where the experimental data were assigned absolute weights by propagation of error on the basis of the following error estimates [6]:

$$\sigma_P = 30\,\mathrm{Pa}, \quad \sigma_\rho = 1.5 \times 10^{-4}\%, \quad \sigma_T = 0.003\,K. \tag{20}$$

A comparison between the experimental P–ρ–T data of Nowak et al. [6] and the values calculated from our equation is presented in Fig. 1 in the form of pressure deviations as a function of the inverse compressibility $\tilde{\chi}_T^{-1}$ along various isotherms. The equation reproduces the data within

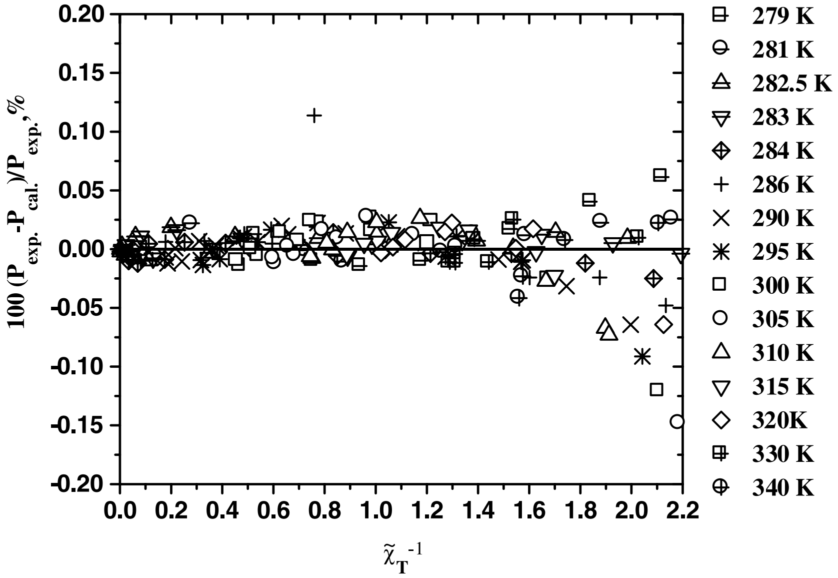

Fig. 1. Percentage differences between the experimental pressure data of Nowak et al. [6] and the values calculated from the crossover model fundamental equation.

the estimated errors. We also note that the average percent deviation in pressure is calculated to be $|\Delta| = \left|\frac{P_{\exp} - P_{\mathrm{calc}}}{P_{\exp}}\right| = 0.016\%$.

We compare the equation of state with the P–ρ–T data obtained by Hasting et al. [21], Douslin and Harrison [22], Trappeniers et al. [23], Michels and Geldermans [24], and those of Thomas and Zander [25]. Comparisons of the three sets of data with the crossover model predictions are given as absolute mean values of the percent deviations of the experimental pressures from the calculated pressures from our formulation. This value was found to be 0.016% for the experimental data of Hastings et al., 0.043% for those of Douslin and Harisson, 0.032% for the data measured by Trappeniers et al., 0.127% for those of Michels and Geldermans and finally this value was 0.087% for the data of Thomas and Zander. It is clear that among the analyzed experimental data, those obtained by Hastings et al. [21] were the most accurate compared to those of Nowak et al. [6].

The analytic background coefficients $\tilde{\mu}_2$ and $\tilde{\mu}_3$ can be best determined from a comparison with speed-of-sound data. The set of experimental data of Gammon [7] and those measured by Dregulyas and Stavtsev [8] are characterized by a wider range of temperatures and densities around the critical point. These latter data were discarded from the determination of the caloric parameters for reasons we will explain later. Therefore, our choice was made to use the speed-of-sound data of Gammon [7].

However, their temperature range was limited. For this purpose, we used the speed of sound data reported by Gammon [7] supplemented with the isobaric specific-heat data of Hejmadi and Powers [9]. The experimental speeds of sound of Gammon and the isobaric specific-heat data have been measured along isobars as a function of temperature. In Figs. 2 and 3, we show these same speed-of-sound and isobaric specific-heat data successively as a function of density when the densities associated with the experimental temperatures and pressures are calculated from the equation of state. We finally made a comparison of our model with another set of speed-of-sound data measured by Dregulyas and Stavtsev [8]. It is seen that the locations of the speed-of-sound minima are reproduced near the critical point. Theory predicts a zero value of sound speed at the critical point. However, we should mention that we have omitted the isotherm 293.15 K for the speed of sound of Dregulyas and Stavtsev [8] from the comparisons due to measured values showing very large departures from our formulation. The final comparison of these data is shown in Fig. 4.

We can also notice in Fig. 3 that the maxima locations of the isobaric specific-heat data obtained by Hejmadi and Powers [9] are somewhat

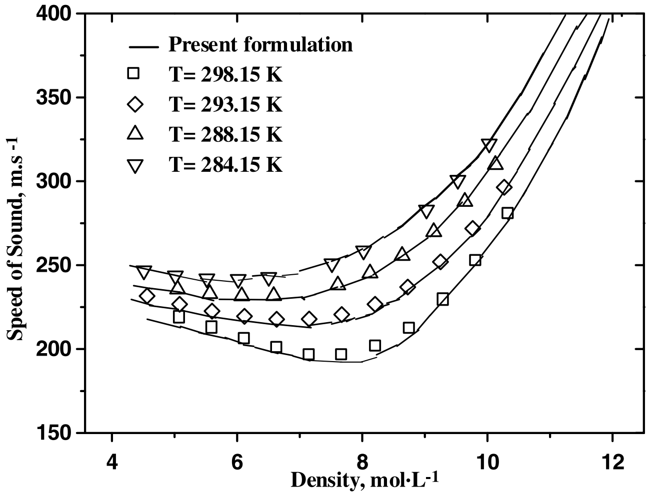

Fig. 2. Speed of sound C_s as a function of density at various temperatures. The data points are experimental values of Gammon [7], and the solid curve represents C_s values calculated from our crossover model fundamental equation.

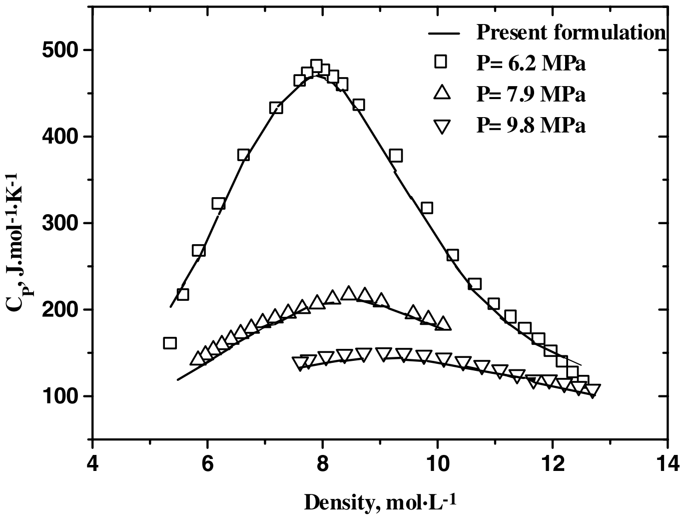

Fig. 3. Isobaric specific heat C_P as a function of density at various pressures. The data points are experimental values of Hejmadi and Powers [9], and the solid curve represents C_P values calculated from our crossover model fundamental equation.

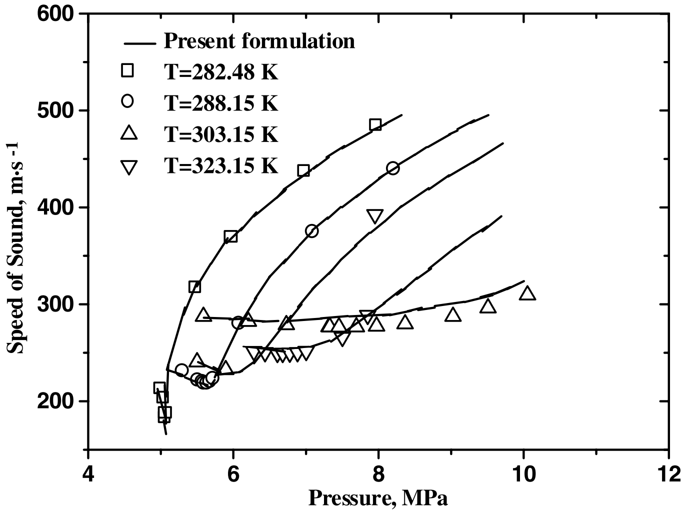

Fig. 4. Speed of sound C_s as a function of pressure at various temperatures. The data points are experimental values of Dregulyas and Stavtsev [8], and the solid curve represents C_s values calculated from our crossover model fundamental equation.

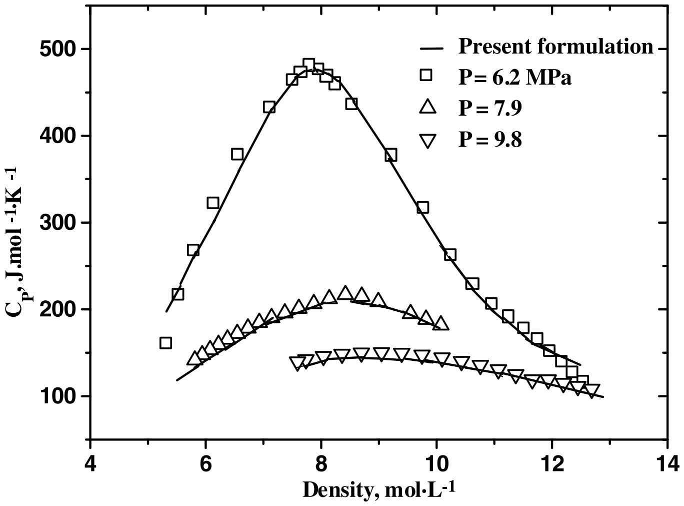

Fig. 5. Isobaric specific heat C_P as a function of density at various pressures. The data points are experimental values of Hejmadi and Powers [9], and the solid curve represents C_P values calculated from our crossover model fundamental equation after a pressure correction of +0.0016 MPa.

shifted from the calculated ones. The apparent critical parameters shift away from the critical density when the critical pressure is approached. Such a behavior is usually a sign that there exists a discrepancy between the critical parameters (T_c, P_c) implied by these specific-heat data and those adopted in the formulation of the present equation of state. We noticed that the problem disappears if the experimental pressures quoted by Hejmadi and Powers [9] are shifted by +0.0160 MPa. The application of this correction has resolved the problem of the isobaric specific-heat data maxima, although we were unable to obtain an independent confirmation from the investigators to justify these corrections. The corrected maxima are shown in Fig. 5.

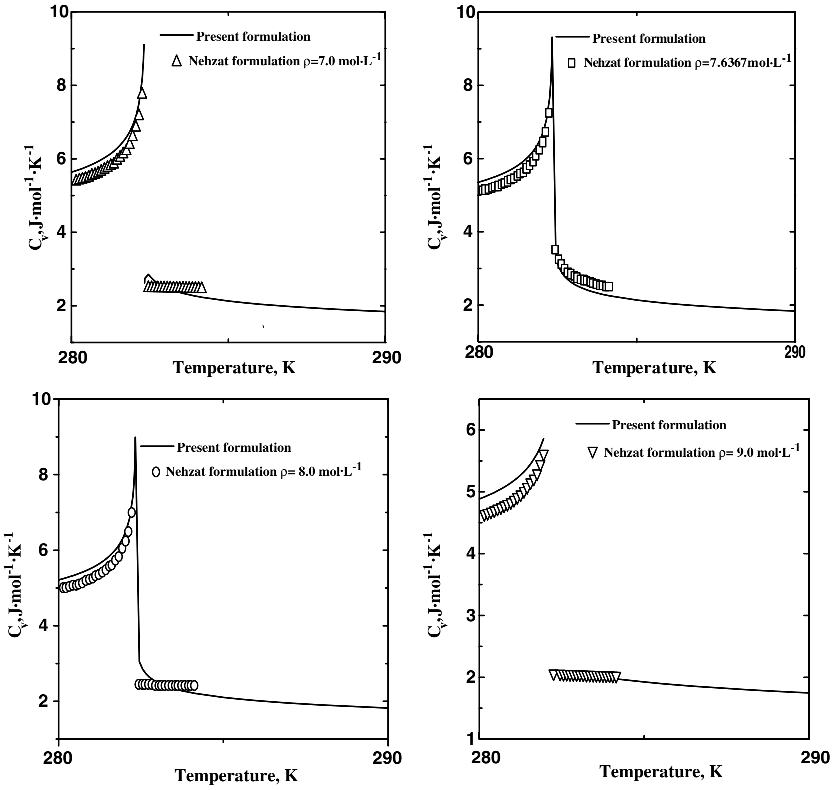

Fig. 6. Isochoric specific heat C_v as a function of temperature corresponding to $\rho =$ 7.0 mol · L^{-1}, $\rho = \rho_c$ = 7.637 mol · L^{-1}, $\rho = 8.0$ mol · L^{-1}, and $\rho = 9.0$ mol · L^{-1}. The data points are the predicted values of C_V from the Nehzat et al. formulation [27], and the solid curve represents C_v values calculated from our crossover model fundamental equation.

A final note concerns the nonanalytic formulation that includes some characteristics of a scaled equation for the thermodynamic properties of ethylene in the critical region that was done by Nehzat et al. [27]. We used the calculated specific heat C_v along different isochores and compared them with those calculated from our formulation as shown in Fig. 6. The equation formulated by Nehzat et al. [27] does not give the correct behavior of C_v along the critical isochore as shown in Fig. 6.

ACKNOWLEDGMENTS

The authors are indebted to J. V. Sengers for encouraging us to submit this work and to Dan Friend and Eric Lemmon of NIST at Boulder, Colorado for sending us all the ethylene data used in this research. The author would like to thank Prof Dr Wagner for sending me the paper containing the ethylene pressure data. The authors also acknowledge the financial support and the computer time that was provided by the ***ANDRU,*** l'Agence Nationale pour le Développement de la Recherche Universitaire of the Algerian Government under the Grant No. Cu 39718.

REFERENCES

1. R. D. McCarty and R. T. Jacobsen, *NBS Tech. Note 1045*, National Bureau of Standards, Washington, DC (1981).
2. R. T. Jacobsen, M. Jahangiri, R. B. Stewart, R. D. McCarty, J. M. H. Levelt Sengers, H. J. White, J. V. Sengers, and G. A. Olchowy, *Ethylene (Ethene)*, *International Thermodynamic Tables of Fluids State* (Blackwell Scientific, Oxford, 1988).
3. J. M. H. Levelt Sengers, G. A. Olchowy, B. Kamgar-Parsi, and J. V. Sengers, A Thermodynamic Surface for the Critical Region of Ethylene, *NBS Tech. Note 1189*, National Bureau of Standards, Washington, DC (1984).
4. J. V. Sengers and J. M. H. Levelt Sengers, *Ann. Rev. Phys. Chem.* **37**:189 (1986).
5. J. V. Sengers and J. M. H. Levelt Sengers, *Int. J. Thermophys.* **5**:195 (1984).
6. P. Nowak, R. Kleinrahm, and W. Wagner, *J. Chem. Thermodyn.* **28**:1423 (1996).
7. B. E. Gammon, presented at the Advisory Committee Meeting of the Joint Industry—Government Ethylene Project, Boulder, Colorado (Dec. 6, 1978).
8. E. K. Dregulyas and A. F. Stavtsev, *Teplofiz. Vysokikh. Temperatur*. **22**:111 (1984).
9. A. V. Hejmadi and J. E. Powers, *Final Report to the Advisory Committee of the Industry-Government Ethylene Project*, Thermal Properties of Fluids Laboratory, University of Michigan, Ann Arbor (1979).
10. Z. Y. Chen, P. C. Albright, and J. V. Sengers, *Phys. Rev. A* **41**:3161 (1990).
11. Z. Y. Chen, A. Abbaci, S. Tang, and J. V. Sengers, *Phys. Rev. A* **42**:4470 (1990).
12. A. Abbaci, Ph.D. thesis, University of Maryland at College Park (1991).
13. P. C. Albright, Z. Y. Chen, and J. V. Sengers, *Phys. Rev. B* **36**:877 (1987).
14. F. W. Balfour, J. V. Sengers, M. R. Moldover, and J. M. H. Levelt Sengers, *Phys. Lett. A* **65**:223 (1978).
15. J. M. H. Levelt Sengers, B. Kamgar Parsi, F. W. Balfour, and J. V. Sengers, *J. Phys. Chem. Ref. Data* **12**:1 (1983).

16. P. C. Albright, T. J. Edwards, Z. Y. Chen, and J. V. Sengers, *J. Chem. Phys.* **3**:1717 (1987).
17. J. F. Nicoll, *Phys. Rev. A* **24**:2203 (1981).
18. J. F. Nicoll and J. K. Bhattacharjee, *Phys. Rev. B* **23**:389 (1981).
19. J. F. Nicoll and P. C. Albright, *Phys. Rev. B* **31**:4576 (1985).
20. J. Smukala, R. Span, and W. Wagner, *J. Phys. Chem. Ref. Data* **29**:1053 (2000).
21. J. R. Hastings, J. M. H. Levelt Sengers, and F. W. Balfour, *J. Chem. Thermodyn.* **12**:1009 (1980).
22. D. R. Douslin and R. H. Harrison, *J. Chem. Thermodyn.* **8**:301 (1976).
23. N. J. Trappeniers, T. Wassenaar, and G. J. Wolkers, *Physica A* **82**:305 (1976).
24. A. Michels and M. Geldermans, *Physica* **9**:967 (1942).
25. W. Thomas and M. Zander, *Int. J. Thermophys.* **1**:383 (1980).
26. M. R. Moldover, *J. Chem. Phys.* **61**:1766 (1979).
27. M. S. Nehzat, K. R. Hall, and P. T. Eubank, *J. Chem. Eng. Data* **28**:205 (1983).